

Multivariate Activation and Connectivity Patterns Discriminate Speech Intelligibility in Wernicke's, Broca's, and Geschwind's Areas

Daniel A. Abrams¹, Srikanth Ryali¹, Tianwen Chen¹, Evan Balaban⁴, Daniel J. Levitin⁴ and Vinod Menon^{1,2,3}

¹Department of Psychiatry and Behavioral Sciences, ²Program in Neuroscience and ³Department of Neurology and Neurological Sciences, Stanford University School of Medicine, Stanford, CA, USA and ⁴Department of Psychology, McGill University, Montreal, QC, Canada

Address correspondence to Daniel A. Abrams and Vinod Menon, Department of Psychiatry and Behavioral Sciences, Stanford University School of Medicine, 401 Quarry Rd., Stanford, CA 94305-5719, USA. Email: daa@stanford.edu (Daniel A. Abrams) and menon@stanford.edu (Vinod Menon).

The brain network underlying speech comprehension is usually described as encompassing fronto-temporal-parietal regions while neuroimaging studies of speech intelligibility have focused on a more spatially restricted network dominated by the superior temporal cortex. Here we use functional magnetic resonance imaging with a novel whole-brain multivariate pattern analysis (MVPA) to more fully characterize neural responses and connectivity to intelligible speech. Consistent with previous univariate findings, intelligible speech elicited greater activity in bilateral superior temporal cortex relative to unintelligible speech. However, MVPA identified a more extensive network that discriminated between intelligible and unintelligible speech, including left-hemisphere middle temporal gyrus, angular gyrus, inferior temporal cortex, and inferior frontal gyrus pars triangularis. These fronto-temporal-parietal areas also showed greater functional connectivity during intelligible, compared with unintelligible, speech. Our results suggest that speech intelligibility is encoded by distinct fine-grained spatial representations and within-task connectivity, rather than differential engagement or disengagement of brain regions, and they provide a more complete view of the brain network serving speech comprehension. Our findings bridge a divide between neural models of speech comprehension and the neuroimaging literature on speech intelligibility, and suggest that speech intelligibility relies on differential multivariate response and connectivity patterns in Wernicke's, Broca's, and Geschwind's areas.

Keywords: Angular gyrus, Auditory cortex, Broca's area, Inferior frontal gyrus, Speech perception

Introduction

Studies investigating the neural basis for sentence-level speech comprehension have highlighted a broad array of brain structures. Classical accounts from neuropsychological evaluations in patients with focal lesions of the cortex have implicated left-hemisphere temporal (Wernicke 1874) and parietal regions (Geschwind 1970) associated with putative Wernicke's and Geschwind's areas for speech comprehension, while other neuropsychological studies have identified prefrontal contributions associated with classically defined Broca's area in the inferior frontal gyrus (IFG; Bates et al. 2003). Functional imaging studies in healthy adults have provided corroborating evidence (Vigneau et al. 2006): left-hemisphere superior temporal cortex (Ben-Shachar et al. 2004) and IFG regions (Friederici et al. 2006) have been implicated in sentence-level syntactic analysis, whereas left inferior parietal cortex regions, most notably the angular

gyrus (AG; Humphries et al. 2006) and Broca's area as well as other subdivisions of the IFG (Rodd et al. 2005), have been implicated in sentence-level semantic processing. Collectively, a distributed left-hemisphere network involving the superior temporal, inferior parietal, and IFG have been implicated in sentence-level speech perception (Tyler and Marslen-Wilson 2008; Peelle, Johnsrude, et al. 2010; Price 2010). Nevertheless, individual studies of speech processing, notably those involving speech intelligibility, have often diverged from these models.

Distinguishing intelligible from unintelligible speech is an influential paradigm for investigating the neural correlates of auditory sentence comprehension. In this approach, brain responses elicited by intelligible speech are examined relative to acoustically matched "unintelligible" speech. Intelligible speech is hypothesized to recruit brain structures supporting phonology, word-form recognition, semantics, and syntax (Scott et al. 2000), while carefully controlled unintelligible speech retains many speech-like qualities (Azadpour and Balaban 2008), including frequency and amplitude modulations and formant-like features, but is not thought to provide direct access to linguistic or semantic representations in the brain.

Imaging studies of speech intelligibility have yielded inconsistent results. Table 1 summarizes the various speech and control stimuli used in this literature as well as the brain regions identified in these studies as a main effect of speech intelligibility. For example, in a seminal positron emission tomography study, results showed that left anterior superior temporal sulcus (aSTS) was sensitive to intelligible speech (Scott et al. 2000), a result which has been corroborated in subsequent functional magnetic resonance imaging (fMRI) studies (Narain et al. 2003; Obleser and Kotz 2010). Other speech intelligibility studies have variably identified additional left-hemisphere regions, including the IFG (Davis and Johnsrude 2003; Eisner et al. 2010; Okada et al. 2010; Davis et al. 2011; McGettigan, Faulkner, et al. 2012) and the AG of the inferior parietal lobe (Davis and Johnsrude 2003; Obleser et al. 2007). In one of these studies, it was shown that activity in left IFG, STS, and AG are correlated with increasing speech intelligibility (Davis and Johnsrude 2003). In contrast, a second study showed that the AG becomes active only during sentence comprehension when the speech signal is sufficiently degraded, and that, consistent with earlier reports (Scott et al. 2000; Narain et al. 2003), sentence processing under more favorable listening conditions is served predominantly by superior temporal cortex (Obleser et al. 2007).

It remains unclear why studies of speech intelligibility have failed to consistently identify main effects of intelligibility in a

Table 1
Summary of previous studies of speech intelligibility

Study	Experimental stimuli	Control stimuli	Univariate analysis and main effect of intelligibility	Multivariate analysis and intelligibility-based classification
Scott et al. (2000)	Normal and noise-vocoded sentences	Spectrally rotated sentences and spectrally rotated/vocoded sentences	Subtraction analysis: Left anterior STS	N/A
Narain et al. (2003)	Normal and noise-vocoded sentences	Spectrally-rotated sentences and spectrally-rotated/vocoded sentences	<i>Subtraction Analysis:</i> Left posterior, mid, and anterior STS (non-contiguous clusters)	N/A
Davis and Johnsrude (2003)	Sentences that were distorted using 3 different methods and 3 levels of distortion		<i>Correlation Analysis:</i> Bilateral MTG, Left hippocampus, Left posterior MTG, Left AG, Left IFG (BA 44), Left SFS, Left precuneus	N/A
Obleser et al. 2007	Sentences of high/low predictability that were noise vocoded at 2, 8, 32 bands		<i>Correlation Analysis:</i> Bilateral STS, Bilateral precuneus, Left MTG, Right MFG, Left SMG	N/A
Obleser and Kotz (2010)	Sentences of high/low predictability that were noise vocoded at 1, 4, 16 bands		<i>Correlation Analysis:</i> Bilateral STS, Left AG	N/A
Adank and Devlin (2010)	Time-compressed sentences	Normal sentences	<i>Subtraction Analysis:</i> Bilateral anterior and posterior STS/STG, Bilateral pre-SMA, Bilateral cingulate sulcus	N/A
Eisner et al. (2010)	"Learnable" noise-vocoded and spectrally-shifted sentences	Spectrally-inverted sentences	<i>Subtraction Analysis:</i> Left IFG (BA 44), Left STS	N/A
Okada et al. (2010)	Normal and noise-vocoded sentences	Spectrally-rotated sentences and spectrally-rotated/vocoded sentences	<i>Subtraction Analysis:</i> Bilateral MTG, Bilateral fusiform gyrus, Left parahippocampal gyrus, Left SMG, Left IFG (BA 45), Left MTG, Right medial temporal lobe, Right cerebellum, Right ITG	ROI-based MVPA: Bilateral Heschl's gyrus, Bilateral anterior and posterior STS, Right mid STS
Davis et al. (2011)	Sentences with 9 levels of signal-correlated-noise		<i>Correlation Analysis:</i> Bilateral anterior and posterior MTG, Bilateral mid STG, Bilateral temporal pole, Left IFG (BAs 44, 45, and 47), Right Heschl's gyrus, Right posterior STG, Left putamen, Bilateral hippocampus, Right amygdala, Left IC, Left fusiform, Left ITG	N/A
McGettigan, Faulkner, et al. (2012a)	High and low-predictability sentences noise-vocoded in 3 bands		<i>Correlation Analysis:</i> Bilateral anterior and posterior STS/STG, Left IFG (BAs 44 and 45), Right IFG (BA 47), Left fusiform gyrus,	N/A
McGettigan, Evans, et al. (2012b)	Dynamic frequency and amplitude variations in sine-wave speech taken from the same original sentence	Dynamic frequency and amplitude variations in sine-wave sentences taken from 2 different sentences	<i>Subtraction Analysis:</i> Bilateral STS, Left IFG (BA 47), Right IFG (BA 45), Left precentral gyrus	ROI-based MVPA: Bilateral STG/MTG, Right inferior occipital gyrus

distributed temporal–frontal–parietal network that is widely accepted in current neural models of speech comprehension. While differences in experimental designs could potentially explain this discrepancy, another possibility is that conventional univariate fMRI methods, which identify voxels in the brain that have larger responses for one stimulus condition relative to another, are unable to distinguish responses in key nodes of the speech comprehension network. An alternative approach is multivariate pattern analysis (MVPA), which identifies spatial patterns of fMRI activity sufficient to discriminate between experimental conditions (Haynes and Rees 2006; Norman et al. 2006; Kriegeskorte and Bandettini 2007). Univariate and MVPA techniques provide complementary information regarding the neural substrates underlying cognitive processes (Schwarzlose et al. 2008). A plausible neurophysiological basis for MVPA is that specific and consistent patterns of neural activity measured across neuronal populations may represent an essential spatial coding mechanism. Moreover, unlike differences in regional signal level, spatial patterns of neural activity have the capacity to represent a large number of stimulus attributes, categories, and cognitive states (Haxby et al. 2001). In support of the utility of MVPA, previous studies of the visual system have shown that multivariate patterns of activity within higher levels of the visual system (i.e. ventral temporal cortex) are more sensitive to category discrimination relative to univariate measures (Haxby et al. 2001).

The vast majority of studies to date have used univariate measures to localize brain regions sensitive to intelligible speech. Only 2 studies have probed speech intelligibility using MVPA (Okada et al. 2010; McGettigan, Evans, et al. 2012). Univariate results in these studies showed that multiple regions of superior temporal and inferior frontal cortex had greater activity for intelligible than unintelligible conditions, and MVPA results showed that bilateral anterior and posterior STG/STS could discriminate between intelligible and unintelligible speech. However, in both studies, MVPA was restricted to the temporal lobe (and an occipital lobe control region in one study: McGettigan, Evans, et al. 2012), and it is currently unknown what additional brain regions discriminate between these speech conditions based on spatial patterns. Given that superior temporal cortex is the only brain region that is consistently identified as showing signal-level differences in univariate studies of speech intelligibility, it may be the case that regions beyond temporal cortex, including the IFG and AG, additionally reflect sensitivity to the intelligibility of speech based on consistent spatial patterns of regional activity.

Here, we use the fMRI data from 20 normal healthy adults and applied a novel whole-brain MVPA to examine this question. We identified 2 goals for the analysis of these data. First, we used a searchlight MVPA (Kriegeskorte et al. 2006; Abrams et al. 2011) to discriminate responses to well-matched intelligible and unintelligible speech conditions and

compared these results with the results from a conventional univariate analysis. Based on the extant literature, we predicted that univariate analysis would reveal signal-level differences in superior temporal cortex for intelligible versus unintelligible speech. Critically, we hypothesized that MVPA would reveal distinct neural representations for these speech conditions in inferior prefrontal and parietal areas known to be important for speech comprehension (Bates et al. 2003). The second goal of this work was to examine functional connectivity between brain regions identified using MVPA and how they are modulated by the intelligibility of speech. The motivation for this analysis is that it addresses whether the coordinated activity across brain regions identified with MVPA characterizes the processing of intelligible speech.

Materials and Methods

Participants

Participants were 20 (11 males) right-handed Stanford University undergraduate and graduate students with no psychiatric or neurological disorders, as assessed by self-report and the SCL-90-R (Derogatis 1992). All participants were native English speakers and were between the ages of 19 and 22 (mean age = 21.2 years). The participants received \$50 in compensation for participation. The Stanford University School of Medicine Human Subjects committee approved the study, and informed consent was obtained from all participants.

Stimuli

Speech stimuli were 23–27 s excerpts of familiar and unfamiliar speeches (e.g. Martin Luther King, President Roosevelt) selected from a compilation of famous speeches of the 20th century (Various 1991). All speech stimuli were digitized at 22 050 Hz sampling rate with 16-bit dynamic range. Consistent with previous reports (Scott et al. 2000; Narain et al. 2003; Okada et al. 2010), we used natural speech sentences (Speech condition) as our intelligible speech condition and spectrally rotated speech stimuli (rSpeech condition; Blesser 1972) as our unintelligible speech condition. To perform spectral rotation on the sentence stimuli, each speech file was low-pass filtered 5 times at 2400 Hz (5-pole elliptical filter, slope 100 dB/octave, max attenuation 60 dB), multiplied by a 2500 Hz sine wave, and low-pass filtered 5 more times at 2400 Hz to prevent aliasing. The original signal and the rotated signal were then each low-pass filtered at 1850 Hz, normalized (largest amplitude set to 1), amplified (largest amplitude set to 8 V) and outputted as wave files. The reason for low-pass filtering at this relatively low frequency (1850 Hz) is that the speech material was taken from a commercial recording of great speeches spanning the 20th century, and the originals (some of which had been recorded in the 1940s) differed in their frequency range. The filtering at 1850 Hz was carried out in order to restrict all of the excerpts to the same frequency range as the excerpt with the narrowest range, so that they would be rendered acoustically comparable. As a further verification, the filtered versions were played for 5 native speakers unfamiliar with the excerpts, and each of these individuals was able to accurately repeat back the text of the speeches.

fMRI Task

Speech and rSpeech stimuli were presented in 2 separate runs each lasting ~7 min; the order of runs was randomized across participants. One run consisted of 18 blocks of alternating Speech, temporally re-ordered Speech, and Rest. The other run consisted of 18 alternating blocks of rSpeech, temporally reordered rSpeech, and Rest. Each stimulus lasted 23–27 s. Data from temporally reordered stimuli were originally included to compare temporal structure processing in speech and music (Abrams et al. 2011) and are not presented here since the goal of the current work study is to examine univariate and multivariate differences in brain response related to speech

intelligibility. The block order and the order of the individual excerpts were counterbalanced across participants. Participants were instructed to press a button on an MRI-compatible button box whenever a sound excerpt ended. All participants reported listening attentively to the speech stimuli. Speech stimuli were presented to participants in the scanner using Eprime V1.0 (Psychological Software Tools, 2002). Participants wore custom-built headphones designed to reduce the background scanner noise to ~70 dBA (Menon and Levitin 2005; Abrams et al. 2011). Because of the temporally extended stimuli used here, fMRI data were acquired during continuous scanning, rather than clustered acquisition sequences preferred for brief auditory stimuli (Gaab et al. 2007; Peelle, Eason, et al. 2010). Given that the background scanner noise was present for both Speech and rSpeech conditions, it is unlikely that scanner noise had a significant influence on the reported results.

fMRI Data Acquisition

Images were acquired on a 3 T GE Signa scanner using a standard GE whole-head coil (software Lx 8.3). A custom-built head holder was used to prevent head movement during the scan. Twenty-eight axial slices (4.0 mm thick, 1.0 mm skip) parallel to the AC/PC line and covering the whole brain were imaged with a temporal resolution of 2 s using a T₂*-weighted gradient-echo spiral in–out pulse sequence (TR = 2000 ms, TE = 30 ms, flip angle = 80°). The field of view was 200 × 200 mm, and the matrix size was 64 × 64, providing an in-plane spatial resolution of 3.125 mm. To reduce blurring and signal loss arising from field inhomogeneities, an automated high-order shimming method based on spiral in–out acquisitions was used before acquiring functional MRI scans (Kim et al. 2000).

fMRI Data Analysis

Preprocessing

The first 2 volumes were not analyzed to allow for signal equilibration. A linear shim correction was applied separately for each slice during reconstruction using a magnetic field map acquired automatically by the pulse sequence at the beginning of the scan (Glover and Lai 1998). The fMRI data were then analyzed using SPM8 analysis software (<http://www.fil.ion.ucl.ac.uk/spm>). Images were realigned to correct for motion, corrected for errors in slice-timing, spatially transformed to standard stereotaxic space (based on the Montreal Neurologic Institute [MNI] coordinate system), resampled every 2 mm using sinc interpolation and smoothed with a 6 mm full-width half-maximum Gaussian kernel to decrease spatial noise prior to statistical analysis. Translational movement in millimeters (x , y , z) and rotational motion in degrees (pitch, roll, yaw) was calculated based on the SPM8 parameters for motion correction of the functional images in each participant. No participants had movement >3 mm translation or 3° of rotation; therefore, none were excluded from further analysis.

Quality Control

As a means of assessing the validity of individual participants' fMRI data, we performed an initial analysis that identified images with poor image quality or artifacts. We find that scrutinizing functional data in this manner is key to ensuring high-quality results. To this end, we calculated the standard deviation of each participant's t -map image for the [Speech – rSpeech] contrast, where the standard deviation is calculated by the sum of the squared distance of each image from the sample mean (VBM toolboxes: <http://dbm.neuro.uni-jena.de/vbm/>). This analysis is based on the assumption that a large standard deviation may indicate the presence of artifacts in the image. The squared distance to the mean was calculated for each participant's data. We used a cut-off of 3 standard deviations to identify outliers. Results revealed no outliers among the 20 participants.

Univariate Statistical Analysis

Task-related brain activation was identified using a general linear model (GLM) and the theory of Gaussian random fields as implemented in SPM8. Individual subject analyses were first

performed by modeling task-related conditions as well as 6 movement parameters from the realignment procedure mentioned above, and regressors were entered separately for each session, with separate columns to account for session effects. Brain activity related to the 4 task conditions (Speech, rSpeech, Reordered Speech, and Reordered rSpeech) was modeled using boxcar functions convolved with a canonical hemodynamic response function and a time derivative to account for voxel-wise latency differences in hemodynamic response. Low-frequency drifts at each voxel were removed using a high-pass filter (0.5 cycles/min) and serial correlations were accounted for by modeling the fMRI time series as a first-degree autoregressive process (Friston et al. 1997). Voxel-wise *t*-statistics maps for each condition were generated for each participant using the GLM, along with the respective contrast images. Group-level activation was determined using individual subject contrast images and a second-level analysis of variance. The 3 main contrasts of interest were [Speech – rSpeech], [Speech – Rest], and [rSpeech – Rest]. We also examined omnibus activation for [Speech + rSpeech] minus [Rest] as well as the contrast [Rest] minus [Speech + rSpeech]. Since rest was an implicit condition in the SPM design matrix, these contrasts were constructed using a value of 0.5 for both Speech and rSpeech in the SPM *T*-contrast vector for the [Speech + rSpeech] minus [Rest] contrast, and a value of –0.5 for the [Rest] minus [Speech + rSpeech] contrast. Significant clusters of activation were determined using a voxel-wise statistical height threshold of $P < 0.005$, with family-wise error corrections for multiple spatial comparisons ($P < 0.05$; 70 voxels) determined using Monte Carlo simulations (Forman et al. 1995; Ward 2000) using a custom Matlab script. Activation foci were superimposed on high-resolution T_1 -weighted images and their locations were interpreted using known functional neuroanatomical landmarks (Duvernoy 1995; Duvernoy and Bourgouin 1999) as has been done in our previous studies (Menon and Levitin 2005; Abrams et al. 2011). Anatomical localizations were cross-validated with the atlas of Mai et al. (2004).

Multivariate Pattern Analysis

A multivariate statistical pattern recognition-based method was used to find brain regions that discriminated between intelligible and unintelligible speech (Abrams et al. 2011) utilizing a nonlinear classifier based on support-vector machine algorithms with radial basis function (RBF) kernels (Muller et al. 2001). Briefly, at each voxel v_i , a $3 \times 3 \times 3$ neighborhood centered at v_i was defined. The spatial pattern of voxels in this block was defined by a 27-dimensional vector. Support vector machine (SVM) classification was performed using LIBSVM software (www.csie.ntu.edu.tw/~cjlin/libsvm). We used an SVM classifier for 4 reasons: first, it is a widely used method in machine learning literature for classification; second, SVM is robust to outliers; third, SVM provides regularization when the number of features is larger than observations; fourth, one can design robust nonlinear classifiers using kernels such as SVM-RBF. For the non-linear SVM classifier, we needed to specify 2 parameters, C (regularization) and α (parameter for RBF kernel), at each searchlight position. We estimated optimal values of C and α and the generalizability of the classifier at each searchlight position by using a combination of grid search and cross-validation procedures. In earlier approaches (Haynes et al. 2007), linear SVM was used and the free parameter, C , was arbitrarily set. In the current work, however, we have optimized the free parameters (C and α) based on the data, thereby designing an optimal classifier. In *M*-fold cross-validation procedure, the data are randomly divided into *M*-folds. *M* – 1 folds were used for training the classifier and the remaining fold was used for testing. This procedure is repeated *M* times wherein a different fold was left out for testing. We estimated class labels of the test data at each fold and computed the average classification accuracy obtained at each fold, termed here as the cross-validation accuracy (CVA). The optimal parameters were found by grid searching the parameter space and selecting the pair of values (C , α) at which the *M*-fold CVA is maximum. In order to search for a wide range of values, we varied the values of C and α from 0.125 to 32 in steps of 2 (0.125, 0.25, 0.5, ..., 16, 32). Here we used a leave-one-out cross-validation procedure where $M = N$ (where N is the number of data samples in each condition/class). The resulting 3-D map of CVA at every voxel was used to detect brain regions that

discriminated between the individual subjects' *t*-score maps for each of the 2 experimental conditions: [Speech – Rest] and [rSpeech – Rest]. Under the null hypothesis that there is no difference between the 2 conditions, the CVAs were assumed to follow the binomial distribution $Bi(N, p)$ with parameters N equal to the total number of participants and p equal to 0.5 (under the null hypothesis, the probability of each condition is equal; Pereira et al. 2009). The CVAs were then converted to *p*-values using the binomial distribution, thresholded for height at $P < 0.05$ and a cluster extent of 50 voxels. While many published results using the “searchlight” MVPA approach have not included any extent thresholding (Haynes et al. 2007; Abrams et al. 2011), we used a 50-voxel extent threshold to eliminate isolated suprathreshold voxels.

Interpretation of MVPA

The results from the multivariate analysis are interpreted in a fundamentally different manner as those described for traditional univariate results. Univariate results show which voxels in the brain have greater magnitude of activation for one stimulus condition (or contrast) relative to another. Multivariate results show whether local patterns of fMRI activity across a predetermined number of voxels (a $3 \times 3 \times 3$ volume of voxels in the current study) discriminate between stimulus conditions, and this is analogous to a population code in near-field responses (Wang et al. 1995). It is critical to note that, unlike the univariate method, MVPA does not provide information about which voxels “prefer” a given stimulus condition relative to second condition. Our multivariate analyses identify the location of voxels that consistently demonstrate a fundamentally different spatial pattern of activity for one stimulus condition relative to another (Haynes and Rees 2006; Kriegeskorte et al. 2006; Schwarzlose et al. 2008; Pereira et al. 2009; Abrams et al. 2011).

Anatomical ROIs

We used the Harvard–Oxford probabilistic structural atlas (Smith et al. 2004) to determine classification accuracies within specific frontal and temporal cortex ROIs. A probability threshold of 25% was used to define frontal and temporal lobe ROIs. To enable a greater level of anatomical specificity for suprathreshold classification accuracies within the parietal lobe (i.e. PGa and PGp), we used probabilistic maps developed based on observer-independent definitions of cytoarchitectonic borders (Caspers et al. 2006).

ROI Analysis

The aim of this analysis was to determine whether voxels that showed suprathreshold classification in the MVPA for [Speech – Rest] versus [rSpeech – Rest] also differed in activation levels. This analysis does not violate rules of non-independence since MVPA results identifying an ROI are ambiguous with regards to whether a univariate difference exists within that ROI. This post-hoc analysis was performed using the 6 left-hemisphere frontal, temporal, and parietal ROIs found in the MVPA, including pars triangularis (BA 45), anterior (aMTG), and posterior middle temporal gyrus (pMTG), posterior inferior temporal cortex (pITC), and PGa and PGp of the AG. This ROI analysis was restricted to voxels that showed suprathreshold classification in the MVPA for [Speech – Rest] versus [rSpeech – Rest]. Within these regions, ANOVAs were used to compare the mean activation levels for the [Speech – rSpeech] contrast. ROI analyses were conducted using the MarsBaR toolbox (<http://marsbar.sourceforge.net>).

Functional Connectivity Analyses

Functional connectivity analyses were conducted by computing the correlation between activation in specific regions of interest. Individual time series were extracted from the IFG (BA 45), aMTG, pMTG, PGa, and PGp voxels within a 6-mm radius of the peak classification accuracy in each of these regions. This analysis was limited to left-hemisphere brain structures whose role in sentence-level speech comprehension has been well described (Tyler and Marslen-Wilson 2008; Peelle, Johnsrude, et al. 2010; Price 2010). Given that current models of speech comprehension have not delineated clear roles for the other brain regions identified with MVPA (e.g. left ITC and right hemisphere AG), these regions were not included in the functional

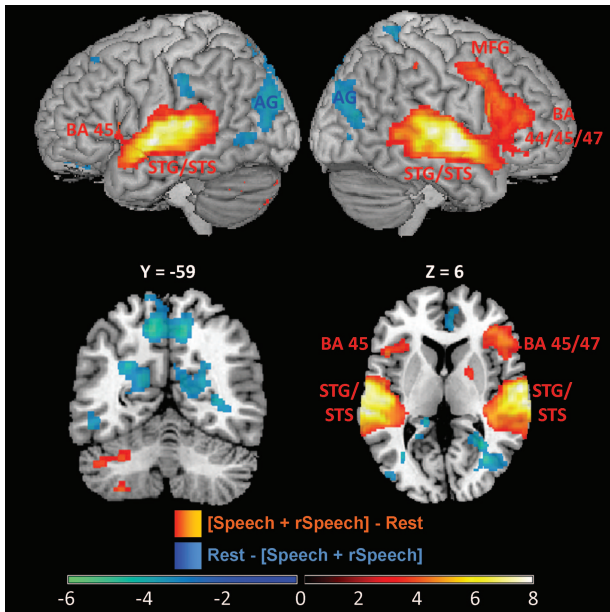


Figure 1. Omnibus responses to Speech and rSpeech. Surface rendering, coronal ($Y = -59$), and axial ($Z = 6$) slices of cortical regions activated during speech and rotated speech conditions (heat map) and deactivated during rest (blue). Images were thresholded using a voxel-wise statistical height threshold of $P < 0.005$, with corrections for multiple spatial comparisons at the cluster level ($P < 0.05$). BA 44, pars opercularis of the inferior frontal gyrus; BA 45, pars triangularis of the inferior frontal gyrus; BA 47, pars orbitalis of the inferior frontal gyrus; AG, angular gyrus; STG, superior temporal gyrus; STS, superior temporal sulcus.

connectivity analysis. For each subject, fMRI time series (1 for each ROI and subject) were averaged separately across voxels within these ROIs after high-pass filtering ($f < 1/120$ Hz) the low-frequency drift. The first 2 TRs of each block were removed from the resulting time series and inter-regional cross-correlation was computed separately for the 2 conditions (Speech, rSpeech). The correlation coefficients between regions i and j , $r_{i,j}$, were transformed to a normal distribution using Fisher's r -to- z transformation: $z_{i,j} = 0.5 \times \ln((1 + r_{i,j}) / (1 - r_{i,j}))$. One-sample t -tests, with Bonferroni corrections for multiple comparisons, were first performed on Z -scores to identify significant network connections in each task condition. Z -scores were exported to SPSS (SPSS Inc., Chicago, IL, USA) and repeated-measures ANOVAs, with factors stimulus condition (Speech, rSpeech) and ROIs, were used to examine between-condition differences in functional connectivity.

Results

Omnibus Responses to Speech and rSpeech

Our first goal was to identify brain structures that showed differential activity in response to the 2 speech conditions compared with rest. We first examined the omnibus GLM results for the [Speech + rSpeech] minus [Rest] comparison to identify brain structures that showed greater activation to the 2 speech conditions compared with rest (Fig. 1, heat map). Activation to the speech conditions was evident throughout bilateral superior temporal cortex and pMTG (Table 2). Superior temporal lobe activation extended from Heschl's gyrus, which contains primary auditory cortex, into posterior auditory association structures, including planum temporale and posterior superior temporal gyrus (pSTG), as well as more anterior structures including planum polare, anterior superior temporal gyrus (aSTG), and the temporal pole.

Table 2

Whole-brain univariate results

Regions	Peak MNI coordinates	Peak Z-score	No. of voxels
Omnibus activation and deactivation			
(A) [Speech + rSpeech] minus rest			
R STG, MTG, IFG, MFG, PCG	64, -6, -4	5.8	8676
L STG, MTG, IFG	-56, -24, 0	5.7	5072
L Cerebellum (lobule VIII, Crus II)	-28, -64, -52	4.1	1064
R SMG	48, -34, 46	3.3	84
R Pallidum	20, 2, 2	3.1	99
R Amygdala	16 -6 -18	3.0	72
(B) Rest minus [Speech + rSpeech]			
L, R Precuneus, LOC	-8 -64 50	4.3	5260
R Postcentral Gyrus	12 -28 46	3.7	514
L Postcentral Gyrus	-6 -32 44	3.7	184
L Temporal Fusiform Gyrus	-36 -36 -14	3.7	456
L Parietal Operculum/SMG	-52 -32 28	3.6	161
R Temporal Fusiform Gyrus	34 -44 -10	3.6	124
R PCG	40 -10 46	3.5	139
L, R Anterior Cingulate	-4 32 -4	3.4	632
L Superior Frontal Gyrus	-18 28 36	3.4	141
L Frontal Pole	-18 42 -16	3.4	229
L SFG / MFG	-24 8 42	3.0	110
Speech versus rSpeech			
(A) Speech minus rSpeech			
L MTG, STG	-64 -6 -10	4.2	1093
R MTG, STG	60 -6 -10	4.1	367
(B) rSpeech minus Speech			
<i>ns</i>			

STG, superior temporal gyrus; MTG, middle temporal gyrus; IFG, inferior frontal gyrus; MFG, middle frontal gyrus; PCG, precentral gyrus; SMG, supramarginal gyrus; LOC, lateral occipital cortex; SFG, superior frontal gyrus.

Activation extended into bilateral IFG, with more extensive activity in the right-hemisphere. Specifically, bilateral pars opercularis (BA 44) and triangularis (BA 45) were activated by the speech conditions relative to rest, with additional activation in right-hemisphere orbital cortex (BA 47), middle frontal gyrus, and frontal pole. Bilateral anterior insulae were also activated as well as right-hemisphere hippocampus, cerebellum, and putamen.

Next, we identified the brain structures that showed "deactivation," that is, more activity for rest compared with the 2 speech conditions by examining the [Rest] minus [Speech + rSpeech] comparison (Fig. 1, blue). Brain structures that showed deactivation included bilateral anterior cingulate (ACC) and right posterior cingulate cortex, separate dorsal and ventral clusters in bilateral precuneus, and bilateral cuneal, fusiform, and angular gyri. Unilateral deactivation was also evident in left anterior supramarginal gyrus and right post-central gyrus.

Univariate Responses to Speech versus rSpeech

Our next goal was to identify brain regions that showed greater activation for the Speech condition relative to rSpeech (Fig. 2; Table 2). Consistent with previous results (Oblaser et al. 2007; Okada et al. 2010), intelligible speech elicited greater activity in bilateral pSTG and aSTG, including extensive activation into the superior temporal sulcus (STS). Moreover, effects of intelligibility were more pronounced in the left-hemisphere relative to the right: activity in the left-hemisphere extended into in the superior temporal plane at the border of the planum temporale and planum polare lateral to Heschl's gyrus and also extended more posteriorly in STG and STS. Importantly, suprathreshold voxels were restricted to auditory association cortex: there were no suprathreshold voxels in either Heschl's gyrus, which contains

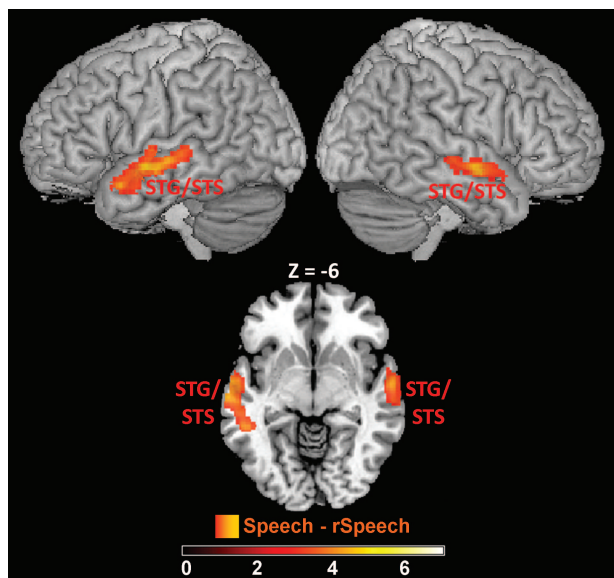


Figure 2. Univariate responses to Speech versus rSpeech. Surface rendering and axial ($Z = -6$) slice of cortical regions with greater activation during intelligible relative to unintelligible speech (the [Speech–rSpeech] contrast). Images were thresholded using a voxel-wise statistical height threshold of $P < 0.005$, with corrections for multiple spatial comparisons at the cluster level ($P < 0.05$). No voxels survived this criteria for the [rSpeech – Speech] contrast. STG, superior temporal gyrus; STS, superior temporal sulcus.

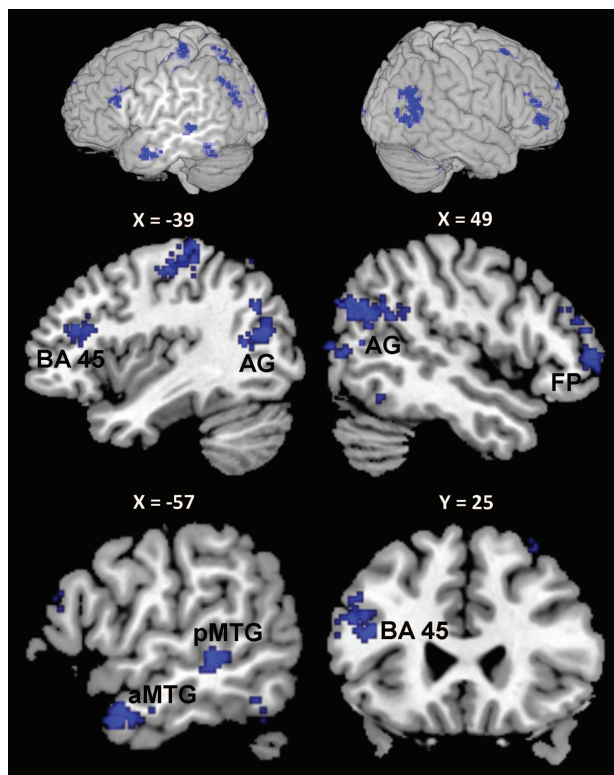


Figure 3. Multivariate pattern analysis of Speech versus rSpeech. Classification maps show brain regions whose activity patterns discriminated between [Speech – Rest] and [rSpeech – Rest] conditions. Maximum classification accuracy ranged from 80% to 85% across all brain regions identified by MVPA. AG, angular gyrus; FP, frontal pole; aMTG, anterior middle temporal gyrus; pMTG, posterior middle temporal gyrus; BA 45, pars triangularis of the inferior frontal gyrus.

Table 3

Multivariate classification accuracy in left-hemisphere ROIs

Cortical Structure	Coordinate of maximum classification accuracy (MNI)	Size (voxels)	Mean classification accuracy (%)	Maximum classification accuracy (%)
BA 45	–44, 28, 16	90	75.3	85.0
aMTG	–56, 6, –28	65	74.4	82.5
pMTG	–60, –34, –6	50	76.7	85.0
pITC	–50, –54, –16	54	74.1	80.0
PGa	–48, –62, 38	47	73.7	80.0
PGp	–38, –70, 20	88	74.1	82.5

primary auditory cortex, or in any other brain regions outside the superior temporal cortex for this contrast. When we examined the [rSpeech – Speech] contrast, no voxels survived our thresholding criteria.

MVPA of Speech versus rSpeech

Our next goal was to examine whether multi-voxel patterns of fMRI activity measured throughout the entire brain were sufficient to discriminate between Speech and rSpeech conditions. MVPA results indicated that distributed brain structures, both within and beyond superior temporal cortex, were able to discriminate between these 2 speech conditions (Fig. 3). In the left-hemisphere superior temporal cortex, 2 separate clusters showed significant discriminability between Speech and rSpeech conditions, with one cluster located in aSTS extending into aMTG and one cluster located in pMTG. A third significant temporal lobe cluster was evident in the temporo-occipital portion of the left pITC. Importantly, there were a number of clusters beyond the temporal cortex. In the frontal lobe, MVPA identified a region of the left inferior temporal gyrus in dorsal pars triangularis (BA 45) that extended into the middle frontal gyrus, as well as 2 clusters in the right-hemisphere frontal pole, and a cluster in the right superior frontal sulcus. In the parietal lobe, suprathreshold classification was also evident in bilateral angular gyrus and precuneus as well as the left hemisphere postcentral gyrus. Suprathreshold classification accuracies within the left AG extended into its 2 cytoarchitectonically distinct anterior (PGa) and posterior subdivisions (PGp; Caspers et al. 2006). Descriptive statistics for classification accuracies in these left-hemisphere brain regions are displayed in Table 3.

Overlap Between Univariate and Multivariate Responses to Speech versus rSpeech

Because GLM and MVPA provide complementary information about the neural substrates of cognitive processes (Schwarzlose et al. 2008), we examined the extent to which results from these analyses revealed overlapping cortical structures. First, we examined overlap between temporal lobe regions identified in the [Speech – rSpeech] GLM and the temporal lobe clusters identified with MVPA. Results indicate that nearly all of the voxels in the pMTG region identified in the MVPA overlap with the GLM results while the aMTG cluster from the MVPA partially overlaps with the anterior-most portion of the GLM results (Fig. 4, green).

Given the partially overlapping left-hemisphere GLM and MVPA results, our next goal was to examine the extent to which signal-level differences between Speech and rSpeech conditions could have been driving MVPA results in the

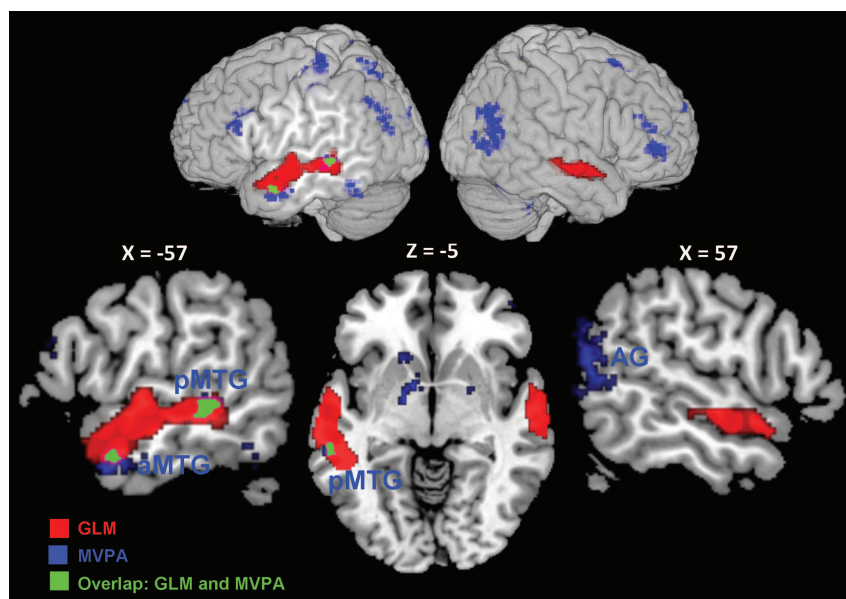


Figure 4. Overlap between univariate and multivariate responses to Speech versus rSpeech. Anterior and posterior left middle temporal gyrus (MTG) regions showed significant overlap in multivariate and univariate responses to speech intelligibility. Outside the left MTG, there was no overlap between the MVPA and univariate results. aMTG, anterior middle temporal gyrus; pMTG, posterior middle temporal gyrus; AG, angular gyrus.

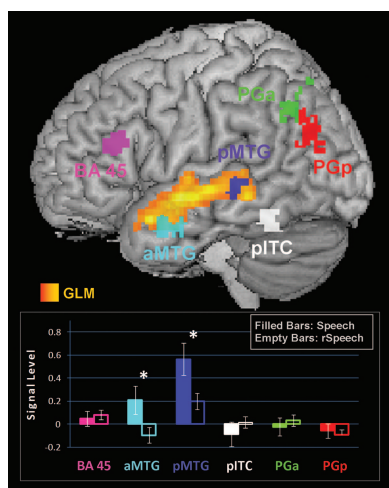


Figure 5. Signal levels in left-hemisphere ROIs. Signal level differences for Speech and rSpeech conditions are plotted in the bar graph for 6 left-hemisphere regions identified by MVPA. The filled and empty bars represent signal levels for the Speech and rSpeech conditions, respectively. Signal-level differences in the anterior and posterior MTG showed significant signal-level differences between Speech and rSpeech; the pars triangularis of the inferior frontal gyrus (BA 45), the posterior inferior temporal cortex (pITC), and the anterior (PGa) and posterior (PGp) regions of the angular gyrus did not differ in signal level.

previously identified clusters. Consistent with the overlapping results in the temporal cortex, results show statistically significant [Speech – rSpeech] signal-level differences for the aMTG and pMTG clusters based on *t*-score average, beta average, and mean signal change measures ($P \leq 0.01$ for all measures in both aMTG and pMTG clusters; Fig. 5). Importantly, signal levels were statistically similar for the [Speech – rSpeech] comparison in all the frontal and parietal nodes as well as the pITC ($P > 0.35$ for all signal level measures in BA 45, pITC, PGa and PGp clusters). This latter finding strongly suggests

that patterns of BOLD activity identified by MVPA in the inferior frontal and parietal clusters were not driven by signal-level differences. We also performed 1-sample *t*-tests on the beta average and the mean signal change for each ROI and stimulus condition combination to examine whether they differed significantly from baseline. Results showed that pMTG had greater activity relative to the baseline for both Speech and rSpeech conditions ($P \leq 0.011$ for both signal level measures and stimulus conditions), while none of the other ROI and stimulus condition combinations had values that differed significantly from baseline ($P > 0.05$ for all other signal level measures and stimulus conditions combinations for BA 45, aMTG, pITC, PGa, and PGp).

Functional Connectivity during Speech and rSpeech

To examine the functional relationships between the brain regions identified using MVPA during the processing of both Speech and rSpeech, we performed a functional connectivity analysis on the time series data from 6-mm spheres centered at the 5 classification peaks (IFG, aMTG, pMTG, PGa, and PGp) collected during these stimulus conditions. For the Speech condition, 9 of the 10 connections ($P = 0.02$, binomial test) between MVPA regions were significantly connected (Fig. 6). In contrast, for the rSpeech condition, only 4 of the 10 connections ($P = 0.75$, binomial test) we examined reached significance (Fig. 6). A direct comparison between Speech and rSpeech conditions using repeated-measures ANOVA with factors stimulus condition (Speech, rSpeech) and ROI (IFG, aMTG, pMTG, PGa, and PGp) revealed a significant main effect of stimulus ($F_{1,19} = 6.553$; $P = 0.019$), with greater connectivity in the Speech, compared with rSpeech, condition. There were no significant interaction between stimulus and ROI ($F_{9,171} = 0.760$; $P = 0.654$).

A recent intrinsic connectivity analysis showed that PGa and PGp have different intrinsic connectivity profiles (Uddin et al. 2010) and it is unknown whether these AG

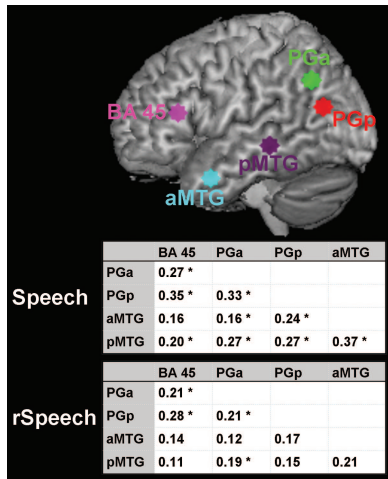


Figure 6. Functional connectivity during Speech and rSpeech. *Top:* The locations of spherical 6 mm ROIs used in the functional connectivity analysis are plotted. The center of these spheres is the voxel associated with peak classification accuracy measured with MVPA within each of these brain regions. *Middle:* Correlation values from the functional connectivity analysis measured in response to the Speech condition. *Bottom:* Correlation values from the functional connectivity analysis measured in response to the rSpeech condition. Overall functional connectivity was greater in the Speech, compared with the rSpeech conditions. Functional connectivity results that met the criteria for significance ($P < 0.005$) are labeled with *. BA 45, pars triangularis of the inferior frontal gyrus; PGa, anterior angular gyrus; PGp, posterior angular gyrus; aMTG, anterior middle temporal gyrus; pMTG, posterior middle temporal gyrus.

regions would also show divergent connectivity profiles in task-based analyses. To more specifically examine whether PGa and PGp subregions of the AG showed differential functional connectivity to other regions of the speech intelligibility network, we performed a post-hoc $2 \times 2 \times 3$ (AG Subregion \times Speech Condition \times Target ROI [IFG, aMTG, pMTG]) repeated-measures ANOVA using the Z-score values for each subject and conditions associated with PGa and PGp connectivity. Results indicated a marginally significant main effect of Speech Condition, with Speech eliciting greater functional connectivity relative to rSpeech ($F_{1,19} = 4.317$; $P = 0.052$). There were no significant differences in functional connectivity between PGa and PGp subregions of the AG ($F_{1,19} = 1.205$; $P = 0.286$).

Discussion

Understanding the neural basis of speech comprehension constitutes a fundamental question in cognitive neuroscience, and despite sustained interest in this topic for over a century (Wernicke 1874), it remains a source of debate. Multiple methodological approaches have identified variable patterns of temporal–frontal–parietal regions for sentence-level speech comprehension, but significant discrepancies remain with respect to the precise brain regions involved in speech intelligibility. To address this issue, we combined univariate, multivariate, and functional connectivity analyses of fMRI data to elucidate brain systems underlying the processing of intelligible speech. Consistent with previous studies (Oleser et al. 2007; Adank and Devlin 2010; Oleser and Kotz 2010; Okada et al. 2010), univariate analysis revealed greater activity for intelligible relative to unintelligible speech in

bilateral superior temporal cortex. In addition, MVPA using novel searchlight methods identified a distributed left-hemisphere network that included anterior and posterior MTG, pITC, pars triangularis region of the IFG, and AG region of the inferior parietal cortex, and overlap between univariate activation and multivariate pattern differences were restricted to the MTG. Our results show that sensitivity to the relative intelligibility of speech is reflected by two distinct mechanisms in the speech-processing network: first, a wide expanse of anterior and posterior superior temporal cortex (Oleser et al. 2007; Okada et al. 2010) responds with univariate signal level differences; and secondly, left BA 45 of the inferior frontal cortex and the PGa and PGp subregions of the AG of inferior parietal cortex respond with distinct spatial patterns of neural activity to different manipulations of speech stimuli. Our findings help explain why previous studies of speech intelligibility (Scott et al. 2000; Narain et al. 2003; Oleser et al. 2007; Oleser and Kotz 2010; Okada et al. 2010) may not have converged on the same brain network as that proposed by current models of speech comprehension (Tyler and Marslen-Wilson 2008; Peelle, Johnsrude, et al. 2010; Price 2010). Crucially, our findings point to greater convergence between these approaches than were previously evident, and suggest that multivariate approaches can help to reconcile differences between the speech intelligibility and comprehension literatures. As discussed below, our findings help bridge a gap between the speech intelligibility literature and current neural models of speech comprehension and provide new insights into the contributions of Wernicke's, Broca's, and Geschwind's areas to speech intelligibility.

Multivariate versus Univariate Analysis of Speech Intelligibility

The first goal of our study was to investigate whether multivariate patterns of neural activity associated with speech intelligibility would more completely identify the distributed network described in recent models of speech comprehension. Consistent with previous reports, bilateral superior temporal cortex showed greater univariate signal levels for Speech compared with rSpeech (Fig. 2). Our results highlight a broader region of temporal cortex compared with an initial report (Scott et al. 2000), but are similar to main effects of speech intelligibility reported in other univariate studies (Oleser et al. 2007; Oleser and Kotz 2010; Okada et al. 2010). Importantly, however, MVPA showed that left-hemisphere aMTG, pMTG, pITC, IFG, and AG were also sensitive to the relative intelligibility of sentences. Our MVPA results are consistent with brain regions identified in a previous study in which behavioral sensitivity to the relative intelligibility of auditory sentences was positively correlated with fMRI activity, revealing a network including bilateral superior temporal cortex, left pITC, IFG, and AG (Davis and Johnsrude 2003).

Our results suggest that subtraction-based analysis of intelligibility data may be limited in its ability to identify the extent of the cortical network underlying the intelligibility of sentence-level speech. Specifically, our results indicate that, based on univariate analysis, intelligible and unintelligible speech similarly activate prefrontal and inferior parietal regions; however, this does not preclude differential involvement of these regions in the processing of intelligible speech.

Consistent with this view, we find that left inferior prefrontal and parietal cortex support intelligible speech processing, and processing in these regions is reflected by spatially distributed patterns of neural activity rather than average activity levels. Importantly, there is a striking overlap between the brain regions identified in our MVPA results and the distributed regions highlighted in a recent meta-analysis of the brain's semantic network (Binder et al. 2009), suggesting that the temporal, frontal, and parietal regions identified in our study may all be engaged in differential semantic-level processing of intelligible, compared with unintelligible, speech despite showing no differences in intensity of activation to these stimuli.

It is important to note that relatively similar study designs and univariate analyses of speech intelligibility data in previous works have seldom revealed consistent results when considering main effects of speech intelligibility (see summary Table 1). For example, the table shows that brain regions such as the left IFG and left inferior parietal cortex are only occasionally identified as a main effect of intelligibility. Many factors may contribute to these inconsistencies, including differences in stimuli, the number of participants used in each study, data acquisition methods (Pelle, Johnsrude, et al. 2010), and data analysis considerations, including the thresholding of univariate results. Results from the current study suggest that the use of new analytic tools, such as whole-brain MVPA, may help resolve some of the inconsistencies in this literature by bringing a new level of sensitivity to the data analysis and highlighting the role of fine-grain distributed neural representations. The methods and approach used here may provide a more complete view of brain systems underlying different aspects of speech and language processing, including targeted studies of speech intelligibility in the context of cochlear implant simulations (Eisner et al. 2010), speech in noise (Davis and Johnsrude 2003), and sine-wave speech (McGettigan, Evans, et al. 2012).

Speech Intelligibility and the Left IFG

MVPA results from the current study identified a dorsal region of pars triangularis of the left IFG as a structure whose pattern of fMRI activity can reliably discriminate between intelligible and unintelligible speech. This region shares extensive connections with auditory regions in the temporal lobe (Romanski et al. 1999) and has been implicated in many aspects of speech comprehension, including phonological (Poldrack et al. 1999), syntactic (Ben-Shachar et al. 2004), and semantic (Wagner et al. 2001) processes. The precise role of the IFG in sentence processing remains unknown; however, recent studies have suggested a role for semantic integration (Oleser and Kotz 2010) and working memory necessary for sentence comprehension (Eisner et al. 2010). Our results are consistent with the view that the left IFG supports semantic and/or syntactic analysis of sentences (Caplan et al. 2008), sequencing of speech input (Gelfand and Bookheimer 2003), or auditory working memory demands imposed by naturalistic sentences over time (Schulze et al. 2010). Although the IFG has been implicated in some studies of speech intelligibility, there is no consensus with respect to its localization to BA 44, 45, and 47 (Table 1). Recent receptor mapping studies have provided new insights into the organization of language regions in the IFG (Amunts et al. 2010). Critically, based on

these studies, our study pin points for the first time the anterior aspects of Broca's area (BA 45a) as the main locus of speech intelligibility in the IFG. Our findings suggest that more targeted investigations of speech processing using MVPA will help to further clarify the role of specific subdivisions of the left IFG in sentence processing.

In the context of these left hemisphere findings, it is interesting to contrast univariate and multivariate response patterns in the right IFG. One initial finding was a surprisingly large response of the right IFG relative to the left in the omnibus activation to Speech and rSpeech, with respect to the resting baseline (Fig. 1). A recent meta-analysis investigating right-hemisphere involvement in sentence-level processing has indicated that right IFG activity is not uncommon and is typically associated with executive functions that are not specific to language function, such as auditory selective attention and working memory (Vigneau et al. 2011). Critically, however, neither univariate nor multivariate response patterns in the right IFG distinguished between speech and rotated speech, further emphasizing the specific contributions of different multivariate patterns in the left IFG to speech intelligibility.

Speech Intelligibility and the Left AG

Given the prominence of the left AG in neural models of speech comprehension (Tyler and Marslen-Wilson 2008; Pelle, Johnsrude, et al. 2010; Price 2010) and language processes (Geschwind 1970; Mesulam 1998), and its ubiquity in studies examining semantic processes (Binder et al. 2009), it has been surprising that speech intelligibility paradigms have not typically identified the AG. As previously mentioned, the AG has been implicated in a parametric study of speech intelligibility in which a positive correlation between the intelligibility of sentences and AG activity was reported (Davis and Johnsrude 2003); however a recent study showed the opposite effect in which AG activity was negatively correlated with sentence intelligibility (McGettigan, Faulkner, et al. 2012). The one subtraction-based intelligibility study that identified the left AG involved an experimental design in which both the intelligibility and semantic predictability of sentence stimuli were varied (Oleser et al. 2007). Results from this manipulation showed that the AG becomes active relative to spectrally rotated speech only when highly predictable sentences are sufficiently acoustically degraded but was not revealed as a main effect of intelligibility. The implication of this result is that the AG is not necessary for speech comprehension under ideal listening conditions, which would appear to contradict the hypothesis that the AG is essential for semantic processing of speech stimuli irrespective of acoustical considerations (Binder et al. 2009). Importantly, the AG intelligibility \times predictability interaction finding shown in the Oleser et al. (2007) study was not replicated in a more recent work using a very similar design (Davis et al. 2011).

Our study helps reconcile discrepancies in the literature summarized above. Critically, we found that despite its deactivation (Binder et al. 1999; Greicius et al. 2003), relative to "rest" baseline, and despite its lack of differential engagement to Speech and rSpeech, the AG was sensitive to the intelligibility of speech based on distinct multivariate patterns of neural activity. Cytoarchitectonic mapping revealed that speech intelligibility effects in the parietal cortex were

localized to the AG (Caspers et al. 2006), with no overlap in the supramarginal gyrus and the intra-parietal sulcus. We show that the AG involvement in the processing of speech intelligibility involves both the PGa and PGp, its cytoarchitecturally distinct anterior and posterior subdivisions (Caspers et al. 2006). The anatomical specificity of speech-related processing in circumscribed regions within the AG have implications for reinterpreting findings in the neuropsychological literature indicating that lesions to the parietal cortex do not always produce speech comprehension deficits (Caplan et al. 1996). Specifically, our results suggest that only parietal lesions localized to the PGa or PGp may impair speech comprehension. Taken together, these results provide a new level of anatomical specificity with regards to speech intelligibility in the human parietal cortex.

Our findings of AG involvement in processing of intelligible speech comprehension is consistent with the view that the AG may be critical for higher-level processing of abstract features of the speech signal (Davis and Johnsrude 2003), and most importantly, its semantic content (Binder et al. 2009; Seghier et al. 2010). We hypothesize that the AG, together with Broca's area, forms a tightly coupled network important for speech comprehension. Consistent with this view, recent anatomical studies have revealed direct white matter pathways between the AG and Broca's area via the superior longitudinal fasciculus in humans and macaques (Makris et al. 2005; Petrides and Pandya 2009) and fMRI studies have highlighted strong intrinsic functional connectivity in this fronto-parietal circuit (Turken and Dronkers 2011).

Functional Connectivity in the Speech Intelligibility Network

The second goal of this work was to examine differential functional connectivity between the nodes identified with MVPA during the processing of intelligible and unintelligible speech. Importantly, we computed functional connectivity by removing the first 4 s of transient changes in each block, thereby capturing temporal correlations within the Speech and rSpeech task blocks that do not reflect transitions between high and low levels of activation. We found significant connectivity between nearly all nodes of the speech intelligibility network during the processing of Speech, with subthreshold connectivity between many of these nodes during the rSpeech condition (Fig. 6). In direct comparisons between Speech and rSpeech conditions, connectivity for intelligible speech was significantly greater than unintelligible speech. This finding is strengthened by the fact that the majority of nodes in this distributed network were identified using MVPA and did not show univariate signal-level differences between conditions, thus avoiding the possibility that functional connectivity results were driven by signal-level fluctuations associated with task on-off states.

Our results demonstrate, for the first time, that processing of intelligible speech drives increased functional connectivity relative to unintelligible speech across the distributed temporal-frontal-parietal network encompassing putative Broca's, Wernicke's, and Geschwind's areas. This is an important finding as it suggests that the coordinated activity across established and distributed nodes of the speech comprehension network is necessary for the processing of intelligible speech, independent of overall changes in task on-off

activation. This finding builds on a previous findings showing significant connectivity between the IFG and AG during the processing of intelligible speech (Eisner et al. 2010). Another previous work reported significant functional connectivity during processing of intelligible speech (Obleser et al. 2007); however, the nodes examined in that analysis included dorso-lateral prefrontal cortex and posterior cingulate cortex, whose roles in speech processing are poorly understood, and did not include temporal lobe structures, whose role in speech processing is well established. Given that our results describe patterns of functional connectivity across a well-described network encompassing left MTG, IFG, and AG, an additional strength of this work is the interpretability of the findings within the context of the broader speech comprehension literature.

Conclusions

We have shown that intelligible speech is processed by distinct spatial patterns of neuronal activity in a distributed cortical network that extends beyond superior temporal cortex and includes the left temporal, frontal, and parietal regions. Our results also show that univariate methods used in many previous intelligibility studies are insensitive to effects outside the temporal lobe, which are manifest as differences in multi-voxel patterns of brain activity. Moreover, functional connectivity between nodes identified with MVPA was greater during the processing of intelligible speech even though most of the regions within the network did not show signal-level differences between intelligible and unintelligible speech. More broadly, our findings help to bridge a gap between speech comprehension and speech intelligibility literatures, and suggest a role for classical Wernicke's, Broca's, and Geschwind's areas in the processing of intelligible speech.

Funding

This work was supported by the National Institute on Deafness and Other Communication Disorders at the National Institutes of Health (grant number F32DC010322) to D.A.A. and 1R21DC011095 to V.M.; National Science Foundation (grant number BCS0449927) to V.M. and D.J.L.; Natural Sciences and Engineering Research Council of Canada (grant numbers 223210, 298612) to D.J.L. and E.B., respectively; and Canada Foundation for Innovation (grant number 9908) to E.B.

Notes

We thank Jason Hom for assistance with data acquisition and Drs Lucina Uddin and Miriam Rosenberg-Lee for critical comments on this work. We are grateful to two anonymous reviewers for their valuable suggestions. *Conflict of Interest:* None declared

References

- Abrams DA, Bhatara A, Ryali S, Balaban E, Levitin DJ, Menon V. 2011. Decoding temporal structure in music and speech relies on shared brain resources but elicits different fine-scale spatial patterns. *Cereb Cortex*. 21:1507–1518.
- Adank P, Devlin JT. 2010. On-line plasticity in spoken sentence comprehension: adapting to time-compressed speech. *Neuroimage*. 49:1124–1132.

- Amunts K, Lenzen M, Friederici AD, Schleicher A, Morosan P, Palomero-Gallagher N, Zilles K. 2010. Broca's region: novel organizational principles and multiple receptor mapping. *PLoS Biol.* 8:1–16.
- Azadpour M, Balaban E. 2008. Phonological representations are unconsciously used when processing complex, non-speech signals. *PLoS One.* 3:1–7.
- Bates E, Wilson SM, Saygin AP, Dick F, Sereno MI, Knight RT, Dronkers NF. 2003. Voxel-based lesion-symptom mapping. *Nat Neurosci.* 6:448–450.
- Ben-Shachar M, Palti D, Grodzinsky Y. 2004. Neural correlates of syntactic movement: converging evidence from two fMRI experiments. *Neuroimage.* 21:1320–1336.
- Binder JR, Desai RH, Graves WW, Conant LL. 2009. Where is the semantic system? A critical review and meta-analysis of 120 functional neuroimaging studies. *Cereb Cortex.* 19:2767–2796.
- Binder JR, Frost JA, Hammeke TA, Bellgowan PS, Rao SM, Cox RW. 1999. Conceptual processing during the conscious resting state. A functional MRI study. *J Cogn Neurosci.* 11:80–95.
- Blesser B. 1972. Speech perception under conditions of spectral transformation. I. Phonetic characteristics. *J Speech Hear Res.* 15:5–41.
- Caplan D, Hildebrandt N, Makris N. 1996. Location of lesions in stroke patients with deficits in syntactic processing in sentence comprehension. *Brain.* 119(Pt 3):933–949.
- Caplan D, Stanczak L, Waters G. 2008. Syntactic and thematic constraint effects on blood oxygenation level dependent signal correlates of comprehension of relative clauses. *J Cogn Neurosci.* 20:643–656.
- Caspers S, Geyer S, Schleicher A, Mohlberg H, Amunts K, Zilles K. 2006. The human inferior parietal cortex: cytoarchitectonic parcellation and interindividual variability. *Neuroimage.* 33:430–448.
- Davis MH, Ford MA, Kherif F, Johnsrude IS. 2011. Does semantic context benefit speech understanding through “Top-Down” processes? Evidence from time-resolved sparse fMRI. *J Cogn Neurosci.* 23:3914–3932.
- Davis MH, Johnsrude IS. 2003. Hierarchical processing in spoken language comprehension. *J Neurosci.* 23:3423–3431.
- Derogatis LR. 1992. SCL-90-R: administration, scoring, and procedures manual. 2nd edition. Baltimore (MD): Clinical Psychometric Research.
- Duvernoy HM. 1995. The human brain stem and cerebellum: surface, structure, vascularization, and three-dimensional sectional anatomy with MRI. New York: Springer-Verlag.
- Duvernoy HM, Bourgouin P. 1999. The human brain: surface, three-dimensional sectional anatomy with MRI, and blood supply. New York: Springer.
- Eisner F, McGettigan C, Faulkner A, Rosen S, Scott SK. 2010. Inferior frontal gyrus activation predicts individual differences in perceptual learning of cochlear-implant simulations. *J Neurosci.* 30:7179–7186.
- Forman SD, Cohen JD, Fitzgerald M, Eddy WF, Mintun MA, Noll DC. 1995. Improved assessment of significant activation in functional magnetic resonance imaging (fMRI): use of a cluster-size threshold. *Magn Reson Med.* 33:636–647.
- Friederici AD, Fiebach CJ, Schlesewsky M, Bornkessel ID, von Cramon DY. 2006. Processing linguistic complexity and grammaticality in the left frontal cortex. *Cereb Cortex.* 16:1709–1717.
- Friston KJ, Buechel C, Fink GR, Morris J, Rolls E, Dolan RJ. 1997. Psychophysiological and modulatory interactions in neuroimaging. *Neuroimage.* 6:218–229.
- Gaab N, Gabrieli JD, Glover GH. 2007. Assessing the influence of scanner background noise on auditory processing. II. An fMRI study comparing auditory processing in the absence and presence of recorded scanner noise using a sparse design. *Hum Brain Mapp.* 28:721–732.
- Gelfand JR, Bookheimer SY. 2003. Dissociating neural mechanisms of temporal sequencing and processing phonemes. *Neuron.* 38:831–842.
- Geschwind N. 1970. The organization of language and the brain. *Science.* 170:940–944.
- Glover GH, Lai S. 1998. Self-navigated spiral fMRI: interleaved versus single-shot. *Magn Reson Med.* 39:361–368.
- Greicius MD, Krasnow B, Reiss AL, Menon V. 2003. Functional connectivity in the resting brain: a network analysis of the default mode hypothesis. *Proc Natl Acad Sci USA.* 100:253–258.
- Haxby JV, Gobbini MI, Furey ML, Ishai A, Schouten JL, Pietrini P. 2001. Distributed and overlapping representations of faces and objects in ventral temporal cortex. *Science.* 293:2425–2430.
- Haynes JD, Rees G. 2006. Decoding mental states from brain activity in humans. *Nat Rev Neurosci.* 7:523–534.
- Haynes JD, Sakai K, Rees G, Gilbert S, Frith C, Passingham RE. 2007. Reading hidden intentions in the human brain. *Curr Biol.* 17:323–328.
- Humphries C, Binder JR, Medler DA, Liebenthal E. 2006. Syntactic and semantic modulation of neural activity during auditory sentence comprehension. *J Cogn Neurosci.* 18:665–679.
- Kim SH, Adalsteinsson E, Glover GH, Spielman S. 2000. SVD regularization algorithm for improved high-order shimming. In: Proceedings of the 8th annual meeting of ISMRM. Denver.
- Kriegeskorte N, Bandettini P. 2007. Analyzing for information, not activation, to exploit high-resolution fMRI. *Neuroimage.* 38:649–662.
- Kriegeskorte N, Goebel R, Bandettini P. 2006. Information-based functional brain mapping. *Proc Natl Acad Sci USA.* 103:3863–3868.
- Mai JK, Assheuer J, Paxinos G. 2004. Atlas of the human brain. Amsterdam: Elsevier.
- Makris N, Kennedy DN, McInerney S, Sorensen AG, Wang R, Caviness VS, Pandya DN. 2005. Segmentation of subcomponents within the superior longitudinal fascicle in humans: a quantitative, in vivo, DT-MRI study. *Cereb Cortex.* 15:854–869.
- McGettigan C, Evans S, Rosen S, Agnew ZK, Shah P, Scott SK. 2012. An application of univariate and multivariate approaches in fMRI to quantifying the hemispheric lateralization of acoustic and linguistic processes. *J Cogn Neurosci.* 24:636–652.
- McGettigan C, Faulkner A, Altarelli I, Obleser J, Baverstock H, Scott SK. 2012. Speech comprehension aided by multiple modalities: behavioural and neural interactions. *Neuropsychologia.* 50:762–776.
- Menon V, Levitin DJ. 2005. The rewards of music listening: response and physiological connectivity of the mesolimbic system. *Neuroimage.* 28:175–184.
- Mesulam MM. 1998. From sensation to cognition. *Brain.* 121(Pt 6):1013–1052.
- Muller KR, Mika S, Ratsch G, Tsuda K, Scholkopf B. 2001. An introduction to kernel-based learning algorithms. *IEEE Trans Neural Netw.* 12:181–201.
- Narain C, Scott SK, Wise RJ, Rosen S, Leff A, Iversen SD, Matthews PM. 2003. Defining a left-lateralized response specific to intelligible speech using fMRI. *Cereb Cortex.* 13:1362–1368.
- Norman KA, Polyn SM, Detre GJ, Haxby JV. 2006. Beyond mind-reading: multi-voxel pattern analysis of fMRI data. *Trends Cogn Sci.* 10:424–430.
- Obleser J, Kotz SA. 2010. Expectancy constraints in degraded speech modulate the language comprehension network. *Cereb Cortex.* 20:633–640.
- Obleser J, Wise RJ, Alex Dresner M, Scott SK. 2007. Functional integration across brain regions improves speech perception under adverse listening conditions. *J Neurosci.* 27:2283–2289.
- Okada K, Rong F, Venezia J, Matchin W, Hsieh IH, Saberi K, Serences JT, Hickok G. 2010. Hierarchical organization of human auditory cortex: evidence from acoustic invariance in the response to intelligible speech. *Cereb Cortex.* 20:2486–2495.
- Peelle JE, Eason RJ, Schmitter S, Schwarzbauer C, Davis MH. 2010. Evaluating an acoustically quiet EPI sequence for use in fMRI studies of speech and auditory processing. *Neuroimage.* 52:1410–1419.
- Peelle JE, Johnsrude IS, Davis MH. 2010. Hierarchical processing for speech in human auditory cortex and beyond. *Front Hum Neurosci.* 4:51.

- Pereira F, Mitchell T, Botvinick M. 2009. Machine learning classifiers and fMRI: a tutorial overview. *Neuroimage*. 45: S199–S209.
- Petrides M, Pandya DN. 2009. Distinct parietal and temporal pathways to the homologues of Broca's area in the monkey. *PLoS Biol*. 7: e1000170.
- Poldrack RA, Wagner AD, Prull MW, Desmond JE, Glover GH, Gabrieli JDE. 1999. Functional specialization for semantic and phonological processing in the left inferior prefrontal cortex. *Neuroimage*. 10:15–35.
- Price CJ. 2010. The anatomy of language: a review of 100 fMRI studies published in 2009. *Ann N Y Acad Sci*. 1191:62–88.
- Rodd JM, Davis MH, Johnsrude IS. 2005. The neural mechanisms of speech comprehension: fMRI studies of semantic ambiguity. *Cereb Cortex*. 15:1261–1269.
- Romanski LM, Tian B, Fritz J, Mishkin M, Goldman-Rakic PS, Rauschecker JP. 1999. Dual streams of auditory afferents target multiple domains in the primate prefrontal cortex. *Nat Neurosci*. 2:1131–1136.
- Schulze K, Zysset S, Mueller K, Friederici AD, Koelsch S. 2010. Neuroarchitecture of verbal and tonal working memory in nonmusicians and musicians. *Hum Brain Mapp*. 32:771–783.
- Schwarzlose RF, Swisher JD, Dang S, Kanwisher N. 2008. The distribution of category and location information across object-selective regions in human visual cortex. *Proc Natl Acad Sci USA*. 105:4447–4452.
- Scott SK, Blank CC, Rosen S, Wise RJ. 2000. Identification of a pathway for intelligible speech in the left temporal lobe. *Brain*. 123(Pt 12):2400–2406.
- Seghier ML, Fagan E, Price CJ. 2010. Functional subdivisions in the left angular gyrus where the semantic system meets and diverges from the default network. *J Neurosci*. 30:16809–16817.
- Smith SM, Jenkinson M, Woolrich MW, Beckmann CF, Behrens TE, Johansen-Berg H, Bannister PR, De Luca M, Drobnjak I, Flitney DE *et al*. 2004. Advances in functional and structural MR image analysis and implementation as FSL. *Neuroimage*. 23(Suppl 1): S208–S219.
- Turken AU, Dronkers NF. 2011. The neural architecture of the language comprehension network: converging evidence from lesion and connectivity analyses. *Front Syst Neurosci*. 5:1.
- Tyler LK, Marslen-Wilson W. 2008. Fronto-temporal brain systems supporting spoken language comprehension. *Philos Trans R Soc Lond B Biol Sci*. 363:1037–1054.
- Uddin LQ, Supekar K, Amin H, Rykhlevskaia E, Nguyen DA, Greicius MD, Menon V. 2010. Dissociable connectivity within human angular gyrus and intraparietal sulcus: evidence from functional and structural connectivity. *Cereb Cortex*. 20:2636–2646.
- Various. 1991. Great speeches of the 20th century. Los Angeles: Rhino Records.
- Vigneau M, Beaucousin V, Herve PY, Duffau H, Crivello F, Houde O, Mazoyer B, Tzourio-Mazoyer N. 2006. Meta-analyzing left hemisphere language areas: phonology, semantics, and sentence processing. *Neuroimage*. 30:1414–1432.
- Vigneau M, Beaucousin V, Herve PY, Jobard G, Petit L, Crivello F, Mellet E, Zago L, Mazoyer B, Tzourio-Mazoyer N. 2011. What is right-hemisphere contribution to phonological, lexico-semantic, and sentence processing? Insights from a meta-analysis. *Neuroimage*. 54:577–593.
- Wagner AD, Pare-Blagojev EJ, Clark J, Poldrack RA. 2001. Recovering meaning: left prefrontal cortex guides controlled semantic retrieval. *Neuron*. 31:329–338.
- Wang X, Merzenich MM, Beitel R, Schreiner CE. 1995. Representation of a species-specific vocalization in the primary auditory cortex of the common marmoset: temporal and spectral characteristics. *J Neurophysiol*. 74:2685–2706.
- Ward BD. 2000. Simultaneous inference for fMRI data. AFNI 3dDeconvolve documentation, Milwaukee (WI): Medical College of Wisconsin.
- Wernicke C. 1874. *Der Aphasische Symptomencomplex*. Breslau: Cohn and Weigert.